CHE MUHAMMAD AIMAN

B. ENG. (HONS) CHEMICAL ENGINEERING

SEPTEMBER 2015

DYNAMICS SEPARATION USING CARBON COMPOSITE METAL ORGANIC FRAMEWORK (CCMs) ADSORBENT

CHE MUHAMMAD AIMAN SYAZWAN BIN CHE MOHD ASRI

CHEMICAL ENGINEERING

UNIVERSITI TEKNOLOGI PETRONAS

SEPTEMBER 2015

Dynamics separation using Carbon Composite Metal Organic Framework (CCMs) Adsorbent

by

Che Muhammad Aiman Syazwan Bin Che Mohd Asri
15597

Dissertation submitted in partial fulfilment
of the requirements for the
Bachelor of Engineering (Hons)
(Chemical Engineering)

SEPTEMBER 2015

Universiti Teknologi PETRONAS,
32610, Bandar Seri Iskandar,
Perak Darul Ridzuan.

CERFICATION OF APPROVAL

Dynamic Separation using Carbon Composite Metal Organic Framework (CCMs) Adsorbent

by

Che Muhammad Aiman Syazwan Bin Che Mohd Asri
15597

A project dissertation submitted to the
Chemical Engineering Programme
Universiti Teknologi PETRONAS
in partial fulfilment of the requirement for the

BACHELOR OF ENGINEERING (Hons)
(CHEMICAL ENGINEERING)

Approved by,

_____
(A.P. Dr Mohd Azmi B. Bustam @ Khalil)

UNIVERSITI TEKNOLOGI PETRONAS

BANDAR SERI ISKANDAR, PERAK

September 2015

CERTIFICATION OF ORIGINALITY

This is to certify that I am responsible for the work submitted in this project, that the original work is my own except as specified in the references and acknowledgements, and that the original work contained herein have not been undertaken or done by unspecified sources or persons.

_____

CHE MUHAMMAD AIMAN SYAZWAN BIN CHE MOHD ASRI

ABSTRACT

Currently, CO2 capture is a topical issue in environmental preservation and sustainable growth in development. This review highlights the recent studies on synthesis and characterization in metal organic framework (Ni-MOF-74) for CO2 capture and also the recent advances in the development of Graphene Oxide functionalized Ni-MOF-74 for CO2 capture. In this study, CO2 adsorption on Nickel-MOF-74 and Nickel-MOF-74-GO were investigated and compared. Fitting in as fascinating class of nano-porous materials, MOFs have been considered potential candidates for CO2 capture due to its capability of adsorption. However, water stability is often considered a big weakness of all kinds of metal-organic framework structures available for now. As such, Ni-MOF-74 does not exhibit such degradation which has a characteristic of strong coordination bond strength and remarkable as one of the highest CO2 uptake capacity among MOFs. Here, Ni-MOF-74 was synthesized by using nickel (II) nitrate, $Ni(NO_3)_2 \cdot 6H_2O$ and 2,5-dihydroxyterephthalte acid in the presence of dimethylformamide (DMF) , ethanol and deionized water under conventional hydrothermal method. Thereafter, Ni-MOF-74 was grafted with graphene oxide (GO). MOF provided a high porosity and reactive centers and GO a dense array of carbon atoms to increase dispersive interactions. The resulting materials showed a significant enhancement in porosity owing to the formation of pores at the interface of GO and MOF crystals. GO oxygen groups were identified as nucleation sites for the formation of the MOF crystals. Characterization techniques applied are Fourier transform infrared (FTIR), thermogravimetry analysis (TGA), field emission scanning electron microscope (FESEM), transmission electron microscope (TEM), and the performance of CO2 adsorption on both MOFs is studied using BET method.

ACKNOWLEDGEMENT

First and foremost, all praises to the Almighty, Allah S.W.T. for His mercy and grace, I was able to complete this project in good health and wellbeing. Next, I would like to sincerely thank you my Supervisor, AP. Dr. Mohamad Azmi bin Bustam @ Khalil who has supervised me throughout my project period. His willingness to guide and advise me had helped me in achieving the goals of my project. Besides, he was constantly supportive of the decisions that I make and always share his knowledge and experiences with me.

On the other hand, I would like to extend my gratitude and appreciation to the postgraduates, Dr Sami Ullah who had guided and taught me in many things throughout my final year project. Without their guidance, it is impossible for me to finish the final year project within the given period.

I also would like to thank my beloved parents and family members starting with my father, Che Mohd Asri Che Ghani and my mother, Suzana bt Hamzah for always giving me moral support from behind and being patient listeners to all my struggles.

Last but not least, thanks to my colleagues, friends and those who involved directly and indirectly towards accomplishing my final year project's objectives. In short, I feel blessed to have successfully completed my final year project and for all help that the aforementioned parties have given me. My final year project only becomes a success with their help.

TABLE OF CONTENTS

CERTIFICATION OF APPROVAL ……. ii

CERTIFICATION OF ORIGINALITY ……... iii

ABSTRACT ……. iv

ACKNOWLEDGEMENT …….. v

TABLE OF CONTENTS …… vi

LIST OF FIGURES ……. vii

LIST OF TABLES ……... ix

CHAPTER 1: INTRODUCTION ……... 1

1.1 Background Study …… 1

1.2 Problem Statement …… 2

1.3 Objectives ……. 3

1.4 Scopes of Study …… 3

CHAPTER 2: LITERATURE REVIEW …… 4

2.1 Metal-Organic Frameworks (MOFs). …….. 4

2.2 (MOFs) / Graphene Oxide composites……. 5

2.3 Dynamic adsorption capacity…… 10

CHAPTER 3: METHODOLOGY …….. 11

3.1 Project Flow Chart ……... 11

3.2 Gantt Chart and Key milestones …….. 12

3.3 Research Methodology……. 13

CHAPTER 4: RESULT AND DISCUSSION ……. 19

4.1 Synthesis of Ni-MOF-74 …….. 19

4.2 Characterization of Ni-MOF-74 and Ni-MOF-74/GO……. 20

CHAPTER 5: CONCLUSION AND RECOMMENDATION ……. 31

5.1 Conclusion …… 31

5.2 Recommendation …….. 31

REFERENCES …… 32

APPENDICES ……. 36

LIST OF FIGURES

FIGURE 2.1	Design and construction of MOF (Jeong, H et al., 2011)	4
FIGURE 2.2	Schematic of the composites synthesis (top) and examples of the chemical species involved in the synthesis along with the resulting composite (bottom, here: MOF-74/GO composite)	7
FIGURE 2.3	M-MOF-74 sample analogs	8
FIGURE 4.1	(a) Ni-MOF-74/GO @ Ni-MOF-74 before being dried in the vacuum oven. (b) Ni-MOF-74 after being dried in the vacuum oven. (c) Ni-MOF-74/GO @ Ni-MOF-74 after being dried in the vacuum oven.	19
FIGURE 4.2	Weight % Temperature of Ni-MOF-74 sample synthesized at 60°C	21
FIGURE 4.3	Weight % Temperature of Ni-MOF-74/GO for 1st batch sample	21
FIGURE 4.4	Weight % Temperature of Ni-MOF-74/GO for 2nd batch sample	22
FIGURE 4.5	SEM of Ni-MOF-74 lab sample – Magnification of (a) 100µm (b) 20µm (c) 5µm (d) 5µm (X. Wu et al. , 201)	23
FIGURE 4.6	SEM of Ni-MOF-74/GO – Magnification of 1st batch (a) 20µm (b) 8µm; 2nd batch (c) 20µm (d) 5µm – Length of Particle (b) (d) 10µm-12µm	24
FIGURE 4.7	SEM images and EDS results of Ni-MOF-74/GO, (a) SEM image with specific EDS points, (b) EDS point mode percentage	25
FIGURE 4.8	EDS spectrum of metal content in Ni-MOF-74/GO	26
FIGURE 4.9	TEM of Ni-MOF-74 lab sample – Magnification of (a) 125k (b) 160k – Horizontal field width of (c) 577.2nm	27
FIGURE 4.10	FTIR Spectra of Ni-MOF-74	29

FIGURE 4.11	FTIR Spectra of Ni-MOF-74/GO	29
FIGURE 4.12	Ni-MOF-74 and Ni-MOF-74/GO Adsorption capacity	30

LIST OF TABLES

TABLE 2.1	Dynamic adsorption capacities of the benchmark MOFs for gaseous contaminants measured in grams of gas per gram of adsorbent. (Britt et al., 2008)	10
TABLE 3.1	Project Gantt chart for FYP I	12
TABLE 3.2	Project Gantt chart for FYP I	12
TABLE 3.3	Lists of apparatus and requirements used in this project	16
TABLE 3.4	List of Characterization Equipments	17
TABLE 4.1	Amount of Ni-MOF-74 Synthesized	20

CHAPTER 1
INTRODUCTION

1.1 Background of Study

Metal–organic frameworks (MOFs) are one of the most discussed materials of the last decade. MOF materials are composed of metal ions or clusters strongly coordinated to organic molecules to form porous one-, two-, or three-dimensional structures. Such a molecular arrangement results in crystalline compounds with a highly porous structure. Basically, the type of metal and organic linker determines the structure and properties of the MOFs.

MOFs are produced and synthesized by hydrothermal or solvothermal techniques in which crystals are gradually grown from a hot solution of metal precursors such as a metal nitrate solution. The hydrothermal method has been used successfully for the synthesis of an enormous number of inorganic compounds and inorganic hybrid material (Chandan Dey, Tanay Kundu, Bishnu P. Biswal, Arijit Mallicka and Rahul Banerjeea, 2013). Solvothermal synthesis technique is useful for growing crystals to the suitable structure as the crystals are growing from hours to days.

The MOFs's characteristics such as large pore volume, ultra-low density, highly adaptable pore functionalities, dynamic and reversible structures make them as a promising candidates for adsorption of CO_2 (Li, Liang et al, 2010). MOFs also have widely used as adsorbents for separation of multicomponent systems, such as O_2 over N_2, CO_2 over CH_4, CO_2 over CO and CO_2 over C_2H_4.

1.2 Problem Statement

Recently, Metal–organic frameworks (MOFs), also known as porous coordination polymers (PCPs), synthesized by assembling metal ions with organic ligands have recently emerged as a new class of crystalline porous materials. The amenability to design as well as fine-tunable and uniform pore structures makes them promising materials for a variety of applications. Controllable integration of MOFs and functional materials is leading to the creation of new multifunctional composites/hybrids, which exhibit new properties that are superior to those of the individual components through the collective behavior of the functional units.

Generally, porous MOFs show microporous characters (o_2 nm) whereas the pore sizes could be tuned from several angstroms to several nanometers by typically controlling the length of the bi- or multipodal rigid organic linkers. In addition, versatile framework functionalities beyond their accessible porosity can arise from the metal components (e.g. magnetism, catalysis), organic linkers (e.g. luminescence, nonlinear optics (NLO), chirality) or a combination of both.

However, the porosity of MOFs is often not fully utilized during adsorption process because of the weak interactions between the walls of MOFs and small gas molecules due to the low density of atoms in MOFs and fully open pore space (Suddik et al. 2006).

Taking into account this drawback, one could hybrid MOFs with other porous materials to form MOF composites, which often result in new or modified properties than that of individual counterparts. The introduction of porous materials in the composites not only favors the dispersive forces and provides extra adsorptive sites (Petit and Bandosz 2009, 2010), but also optimizes the pore diameter and creates additional porosity (Petit et al. 2011; Rallapalli et al. 2013), resulting in higher gas adsorption uptake than that of the parent materials.

1.3 Objective

This project will focus on the development of synthesis, characterization and modification of the potential candidate, metal organic framework, Ni-MOF-74 and metal organic framework (MOFs)/ Graphene Oxide composite, MOF-74/GO for CO_2 adsorption.

The two main objectives for this study are as follow:

i. To characterize the synthesized samples of Ni-MOF-74 and Ni-MOF-74/GO via FTIR, TGA, FESEM and TEM.

ii. To study the performance of CO_2 dynamic adsorption on samples, MOF-74 (m-Ni) and Ni-MOF-74/GO using BET.

1.4 Scope of Study

The three main scope of study for this research will be:

i. Study and familiar with the experimental procedure on synthesizing metal organic frameworks, Ni-MOF-74 and modified MOF-74/GO.

ii. Study on performance dynamic adsorption up to 1 bar of Ni-MOF-74 and modified MOF-74/GO.

iii. Study on the CO_2 adsorption capacity of the two metal organic frameworks, Ni-MOF-74 and modified Ni-MOF-74/GO.

CHAPTER 2
LITERATURE REVIEW

2.1 Metal-Organic Frameworks (MOFs)

Recently, metal–organic frameworks (MOFs) have been evaluated as promising CO_2 capture adsorbents due to their extremely high surface area, giant pore volume and tunable pore size. It has been reported that many MOFs have higher CO_2 uptakes than traditional adsorbents under both high pressures and atmospheric pressures (Millwar and Yaghi 2005; Liewellyn et al. 2008; Furukawa et al. 2010; Liu et al. 2010; Yazaydin et al. 2009). MOFs is claimed to be a more efficient, energy-saving, and environmentally alternative for gas separation in the industry (Rong et al., 2009).

MOF materials generally consist of three dimensional organic-inorganic hybrid networks formed by metal based nodes (e.g. Al3+, Cr3+, Cu2+, or Zn2+) bridged by organic linking groups (e.g. carboxylate, pyridyl) principally through coordination bonds. Due to the strong coordination bonds, MOFs are geometrically and crystallographically welldefined framework structures. MOFs can be tuned and designed systematically based on changing the nature of organic linker and/or changing the connectivity of the inorganic moiety and how the building blocks come together to form a net as shown in Figure 2.1.

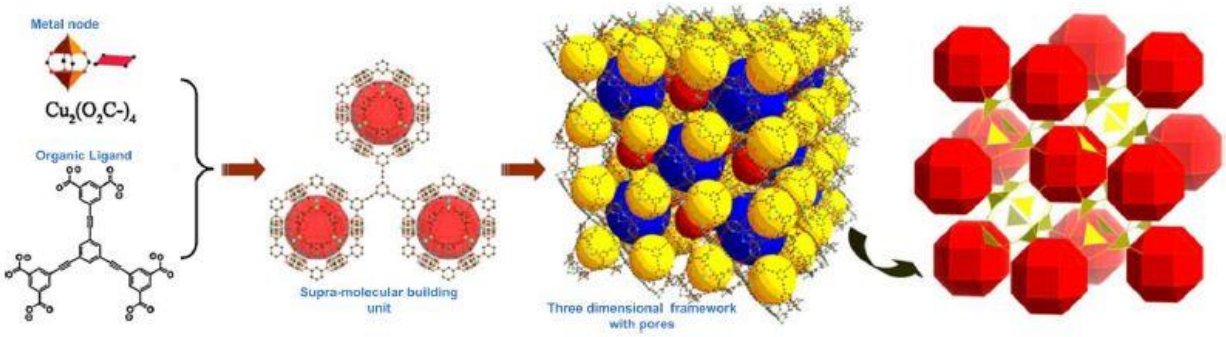

Figure 2.1 Design and construction of MOF (Jeong, H et al., 2011)

This remarkable and easy tunability of MOFs is a key feature that distinguishes these materials from traditional porous materials, such as zeolites and activated carbon. In addition, it allows the optimization of the pore dimension and surface chemistry within metal-organic frameworks that was previously absent in zeolite materials. (Li, Liang et al, 2010)

However, the porosity of MOFs is often not fully utilized during adsorption process because of the weak interactions between the walls of MOFs and small gas molecules due to the low density of atoms in MOFs and fully open pore space (Suddik et al. 2006). Besides, the low mechanical stability and fine powder of MOFs obtained from traditional MOFs synthesis reactions (e.g. solvothermal methods) are not necessarily the best configuration for the applications outlined above. Taking into account this drawback, one could hybrid MOFs with other porous materials to form MOF composites, which often result in new or modified properties than that of individual counterparts.

The introduction of porous materials in the composites not only favors the dispersive forces and provides extra adsorptive sites (Petit and Bandosz 2009, 2010), but also optimizes the pore diameter and creates additional porosity (Petit et al. 2011; Rallapalli et al. 2013), resulting in higher gas adsorption uptake than that of the parent materials.

2.2 (MOFs) / Graphene Oxide composites

MOFs have naturally become prime candidates for gas separation due to large porosity of 3D networks. In addition, the metallic sited provide catalytic properties that have exploited in several reactions (Lee J., et al., 2009). Despite these interesting features, some MOFs still exhibit weak points that have hinder their large-scale deployment.

For instance, poor water stability, although improved in the past years, remains a major concern and causes the collapse of the materials with loss of crystallinity (Schoenecker, P. et al., 2012). This is often attributed to the fragile nature of the metal/ligand junctions. In addition, because of their organic component, MOFs are less

thermostable than their structural cousins, i.e. zeolites, with typical decomposition temperatures ranging between 300 and 500 °C.

Building MOF-based composites is the best approach to address the above mentioned challenges. Two recent reviews broadly describe the formation and applications of a variety of MOF-based composites (I. Ahmed, et al., 2014). These composites take various forms such as: (i) metallic, metal oxide or polyoxometalate nanoparticles dispersed on a MOF's surface, (ii) polymer-impregnated MOFs and (iii) MOF/porous substrate composites.

2.2.1 Graphene Oxide compounds synthesis

For the preparation of MOF composites where MOFs are in a continuous phase, a wide variety of methods have been applied. The methods can be generally categorized into a few major classes. In one of these methods, MOF precursors are mixed with presynthesized composing materials and then the synthesis procedure is carried out. MOF/ Graphene Oxide (MOF/GO) is one of these types of materials that has been widely reported for various applications.

Bandosz et al. published several reports on GO/MOF composites prepared using this procedure and successfully applied them in gas phase adsorptive removal of toxic gases such as NH_3, H_2S, NO_2, and so on. Graphene Oxide was synthesized either via the Hummers method or the Brodie method depending on the composites.

Both involved the oxidation of graphite using strong oxidizing agents, which resulted in the incorporation of oxygen groups. Specifically, epoxy and hydroxyl groups were formed on the surface of the graphene layers while carbonyl and carboxylic groups were found at the edges of the basal planes (W. Gao, et al,. 2009).

A scheme of the synthesis procedure is provided in Fig. 2. First, the MOF precursors, i.e. the metallic salt or metal and the organic ligand, were mixed with the solvents typically employed to synthesize the pure MOF. After a complete dissolution, the graphene component was added, in the form of graphite, GO or aminated GO, depending on the composite. The amount of graphene-based compound added was selected so that its content in the final composites ranged from 5 wt% to 55 wt%

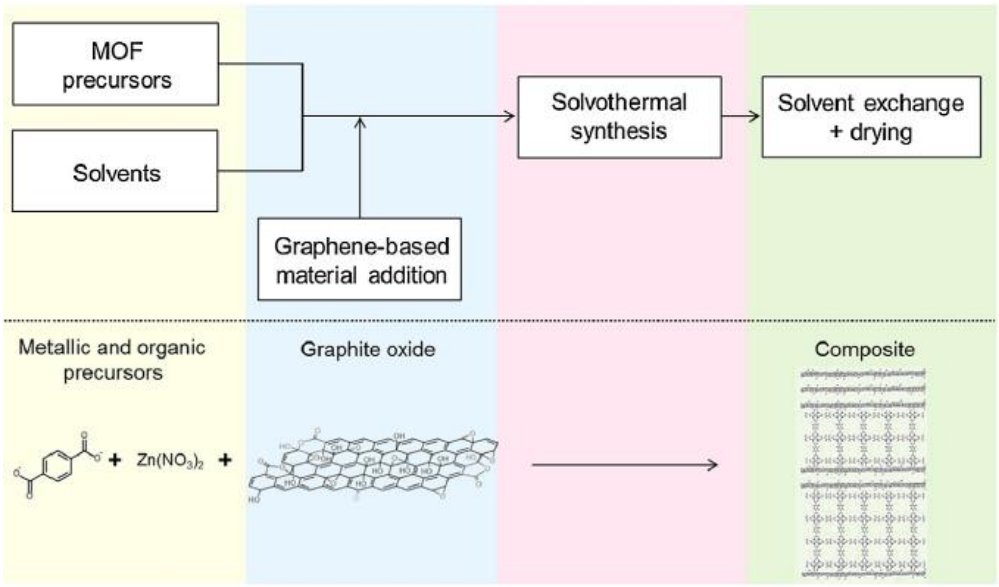

Figure 2.2 Schematic of the composites synthesis (top) and exzmples of the chemical species involved in the synthesis along with the resulting composite (bottom, here: MOF-74/GO composite)

2.2.2 MOF-74

Metal organic frameworks are materials constitute of different metal ions linked by multi-functional organic linkers into one, two or three dimension structures (Gargiulo et al., 2014; Sabouni, 2013). MOF-74 structure is made of organic linker, 2,5-dihydroxyterephthalte linkers. The solvent molecule (water or DMF) can be easily removed under vacuum, increasing the concentration of of unsaturated coordinative metal cations. Among the current MOF structures, MOF-74 presents more co-ordinately unsaturated metal sites that can provide extra number of binding sites to gas molecules (Glover et al., 2010; Wu et al., 2013). Excellent results in CO2 capacity and high selectivity of CO2/CH4 by MOF-74 were obtained from experiments (Liu et al., 2012).

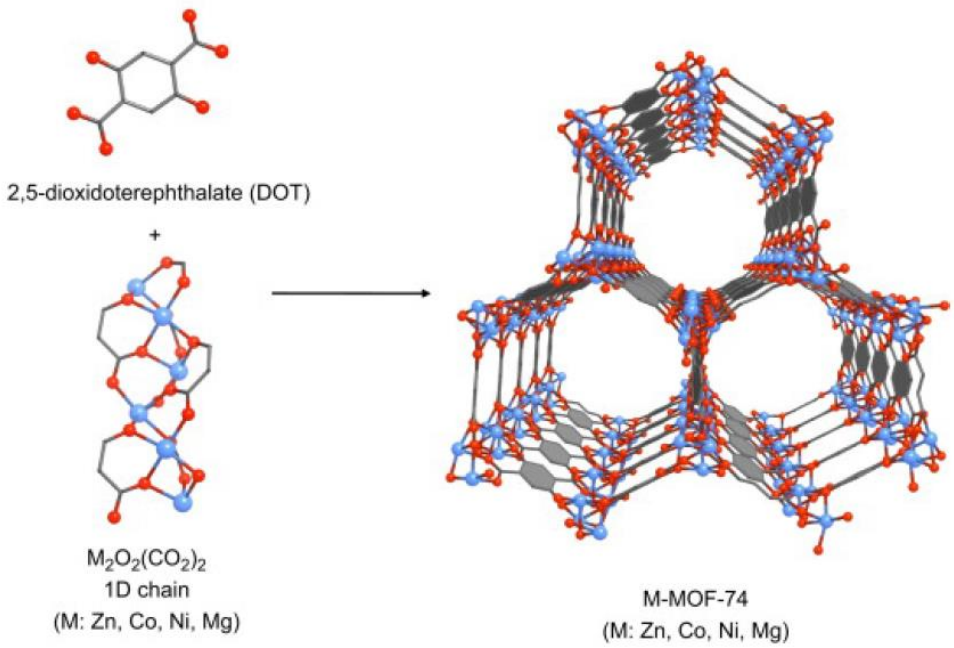

Figure 2.3 M-MOF-74 sample analogs

2.2.3 Synthesis of Nickel-MOF-74 (Ni-MOF-74)

The solution for Ni-MOF-74 was prepared by dissolving a mixture of $Ni(NO_3)_2.6H_2O$ (1.902 g, 6.54 mmol) and DOT (0.382 g, 1.92 mmol) under sonication in a 1:1:1 (v/v/v) mixture of DMF (53.3 mL), ethanol (53.3 mL), and water (53.3 mL).

For the conventional hydrothermal method synthesizing Ni-MOF-74 (1), a homogeneous solution was evenly transferred to two 180-mL Teflon lined stainless-steel autoclaves, about 160 mL each. The autoclaves were capped tightly and heated to 373 K with a heating rate of 5 K/min in an oven. After the reaction under the autogenous pressure for 24 h, the sample was then removed from the oven and allowed to cool to the room temperature. The mother liquor was then carefully decanted from the product and replaced with methanol. Fresh methanol was used to exchange the DMF for 3 days at room temperature. The final product was then isolated by filtration and washed thoroughly with methanol.

2.3 Dynamic adsorption capacity

Although application of MOFs to high-density gas storage has been well studied, virtually no work has been undertaken to measure their capacity for dynamic gas-adsorption properties. Equilibrium adsorption does not adequately predict selectivity, because dynamic capacity is influenced strongly by the kinetics of adsorption. The kinetic properties of adsorption in MOFs have been largely unexamined. For these reasons it is necessary to calculate the dynamic adsorption capacity, which is defined as the quantity of a gas adsorbed by a material before the time at which the concentration of the gas in the effluent stream reaches an arbitrary ‘‘breakthrough’’ value, 5% of the feed concentration in this project. Estimated dynamic adsorption capacities for gaseous contaminations are presented in Table 1.

Table 2.1 Dynamic adsorption capacities of the benchmark MOFs for gaseous contaminants measured in grams of gas per gram of adsorbent. (Britt et al., 2008)

Gas	MOF-5	IRMOF-3	MOF-74	MOF-177	MOF-199	IRMOF-62	BPL carbon	Improvement factor*
Sulfur dioxide	0.001	0.006	0.194†	<0.001	0.032	<0.001	0.033	5.88
Ammonia	0.006	0.105†	0.093	0.042	0.087	0.023	0.001	105
Chlorine	‡	0.335†	‡	<0.001	0.036	0.092	0.190	1.76
Tetrahydrothiophene	0.001	0.007	0.090	<0.001	0.351†	0.084	0.123	2.85
Benzene	0.002	0.056	0.096	0.001	0.176†	0.109	0.155	1.14
Dichloromethane	<0.001	0.001	0.032	<0.001	0.055†	0.019	0.053	1.04
Ethylene oxide	0.001	0.002	0.110	<0.001	0.095†	0.011	0.010	9.50

*Expresses the ratio of dynamic adsorption capacity of the best-performing MOF (†) to that of BPL carbon.
†Best-performing MOFs.
‡Experiments were not performed because of corrosion of the apparatus by chlorine.

CHAPTER 3

METHODOLOGY

3.1 Project Flow Chart

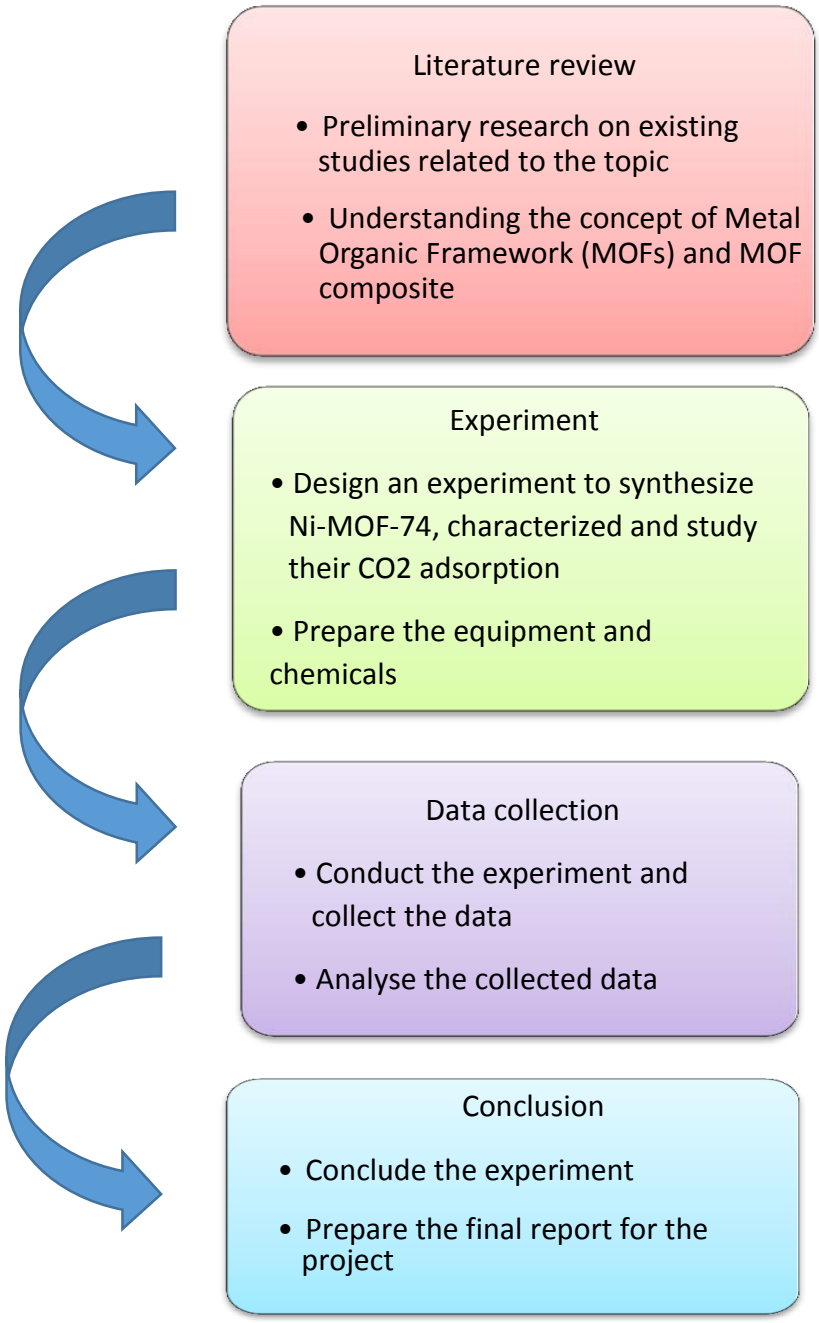

3.2 Gantt Chart and Key milestones

TABLE 3.1: Project Gantt chart for FYP I

Details	Week													
	1	2	3	4	5	6	7	8	9	10	11	12	13	14
Selection of project topic														
Preliminary research work														
Submission of extended proposal						*								
Proposal defence														
Project work continues i. Synthesis of m-MOF-74 ii. Sample preparation for extraction iii. Synthesis MOF/GO														
Submission of interim draft report												*		
Submission of interim report													*	

TABLE 3.2: Project Gantt chart for FYP II

Details	Week														
	1	2	3	4	5	6	7	8	9	10	11	12	13	14	15
Project work continues i. Characterization of MOF-74 (TGA, FTIR, TEM, FESEM, BET) ii. Synthesis of MOF-74/GO															
Submission of progress report							*								
Project work continues i. Characterization of MOF-74/GO (TEM, FESEM, BET, TGA, FTIR)															
Pre-SEDEX										*					
Submission of draft final report											*				
Submission of dissertation (soft bound)												*			
Submission of technical paper												*			
Viva													*		
Submission of project dissertation (Hard Bound)															*

Legends

Project work

* Key Milestone

3.3 Research Methodology

3.3.1 Sample Preparation of Ni-MOF-74

1) 1.902g of Ni $(NO_3)_2 \cdot 6H_2O$, 0.382g of 2,5-dihydroxyterephthalte acid are weighed and placed inside a beaker.

2) A mixture in a ratio of 1:1:1(v/v/v) of DMF (53.5mL), ethanol (53.5mL) and deionized water (53.5mL) is prepared.

3) Ni $(NO_3)_2 \cdot 6H_2O$ and 2,5-dihydroxyterephthalte acid mixture is dissolved in the mixture of DMF, ethanol and deionized water under sonication for about half an hour.

4) The homogeneous solution is evenly transfers to two 180-mL Teflon lined stainless-steel autoclaves, about 160mL each.

5) The autoclaves are caps tightly and heat to 373K with a heating rate of 5K/min in an oven for 24 hours.

5) The mixture is cooled down to room temperature and the mother liquor is removed and replaced with methanol once per day over next three days.

6) Mixture is then evaporated using different temperatures, 60˚C for an hour and 110˚C for 10 hours to result in yellow microcrystalline powder. Small portion of the powder is taken from each temperature for characterization purpose.

7) The sample is heated under vacuum to 80˚C for 5 hours.

8) The sample is left to cool down to room temperature and stored.

3.3.2 Experimental Procedure Flow Chart

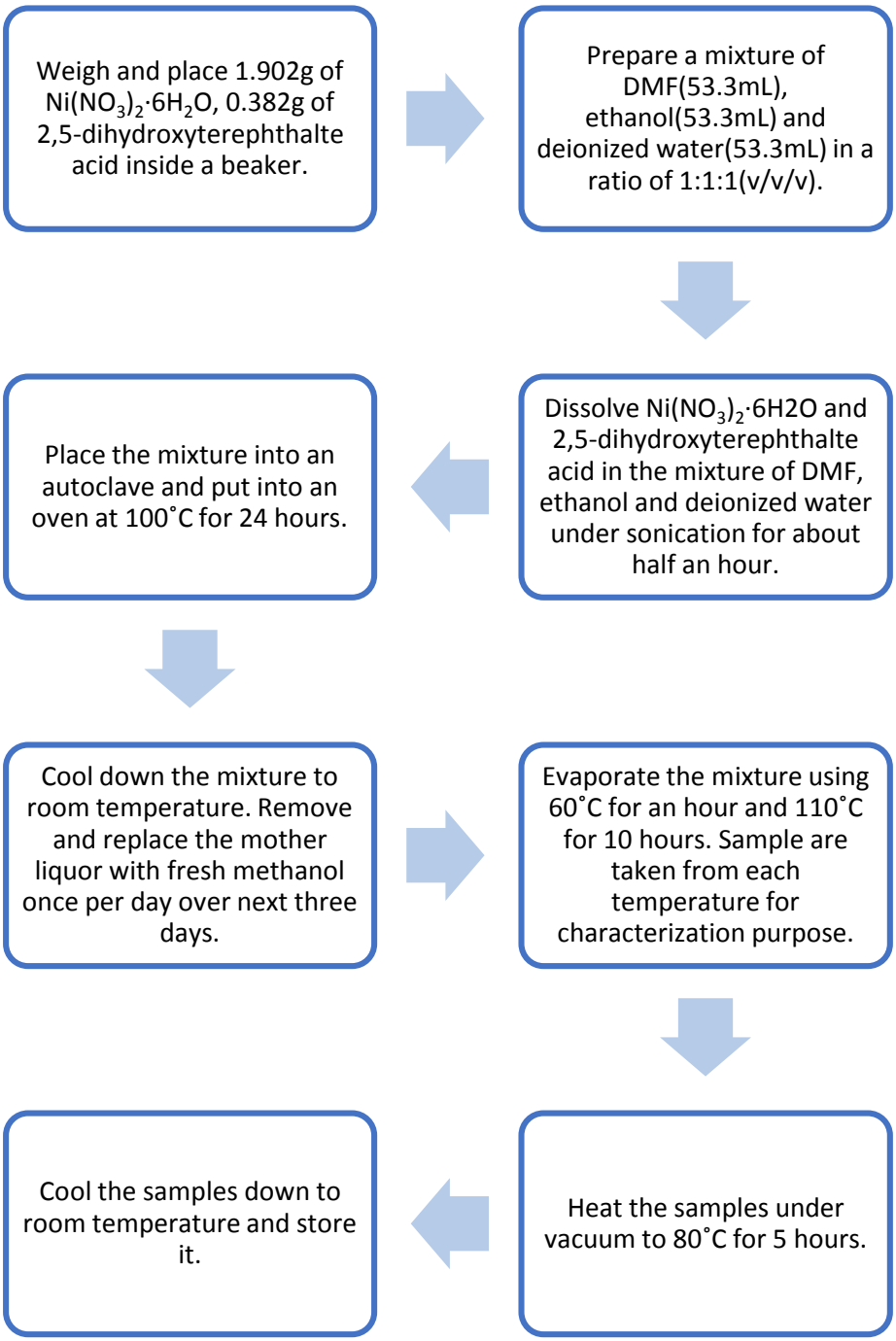

3.3.3 Sample Preparation of Ni-MOF-74/GO

1) The content of GO in the composite was 10 wt. % of the parent MOF. Ni $(NO_3)_2 \cdot 6H_2O$ (1.902 g), 2,5-dihydroxyterephthalte acid (DHTA) (1 g) and graphite oxide (0.05g) was dissolved in N, N-dimethylformamide (DMF, 53.5mL), ethanol (53.5mL) and deionized water (53.5mL).

2) The mixture was sonicated for 30 min, then transferred into 100 ml teflon lined stainless-steel autoclave, reacted for 10 h under 100 ℃ in thermostatic drying oven.

3) After cooling to room temperature, the mother liquor was decanted. The product was washed by ethanol repeatedly, and then dried at room temperature.

3.3.4 Reagent and Chemicals

List of chemicals that are used in the experiement:

- Nickel (II) nitrate hexahydrate, $Ni(NO_3)_2.6H_2O$
- 2,5-dihydroxyterephthalic acid (DHTA)
- N,N-Dimethylformamide
- Methanol
- Sulfuric acid (H_2SO_4)
- Deionized Water
- Ethanol
- Graphene Oxide

3.3.5 Apparatus & Equipments

Below are the lists of apparatus and equipments used in this project.

Table 3.3: Below are lists of apparatus and requirements used in this project

List	***Apparatus***	***Function***
1.	Beaker	To hold chemicals and reagents.
2.	Spatula	To transfer chemicals and reagents from bottle to beakers.
3.	Weighing machine	To measure the weight of chemicals in solid form required for MOF-74 synthesis.
4.	Measuring cylinder	To measure the weight of chemicals in liquid form accurately.
5.	Pipette	To measure liquid in less than 10ml.

Table 3.4: List of Characterization Equipments

Equipment	*Function*
Thermal Gravimetry Analyzer (TGA)	To determine the weight change of a material with temperature change. To find out degradation temperature.
Fourier Transform Infrared Spectroscopy (FTIR)	To identify unknown materials, determine the quality of a sample and quantity of components in a mixture.
Transmission Electron Microscope (TEM)	To observe the compound's morphology and porosity at nano-crystal level.
Scanning Electron Microscopy (SEM)	To observe small structures on the surface of cells and material.

3.3.6 Characterization Techniques

TGA Analysis

Thermogravimetric Analysis (TGA) was carried out in a 100ml/min flowing air atmosphere at a heating rate of 10˚C/min from the temperature of 50˚C to 200˚C using Perkin Elmer Pyris 1 Thermal Gravimetric Analyzer. Degradation temperature of the samples could be observed from the TGA profile.

FTIR Analysis

Fourier Transform Infrared (FTIR) spectrum was obtained from Nicolet FTIR Impact 400 system. About 2mg of the lab samples were grounded with 460 mg of potassium bromide (KBr) under atmosphere. The mixture was then transferred to a die kit and pressed into a pellet. This analysis technique was used to identify unknown materials, determine the quality of the samples and quantity of components in the samples.

TEM Analysis

Zeiss Libra 200 Transmission Electron Microscope (TEM) was used to analyze the geometry and chemical of Ni-MOF-74 particles at atomic level. The TEM instrument was operated at 200 kV. The general morphology of the samples of MOFs was studied for individual nanocrystals.

SEM Analysis

The crystal morphology of the samples was observed using a Zeiss Supra55 Variable Pressure Scanning Electron Microscope (VPSEM). The VPSEM instrument is operated at an accelerating voltage of 2kV.

CHAPTER 4

RESULT AND DISCUSSION

4.1 SYNTHESIS OF Ni-MOF-74

After the synthesis of Ni-MOF-74 and Ni-MOF-74/GO at rate of Ni-MOF-74, the observation has been made. The quantity of Ni-MOF-74 and Ni-MOF-74/GO at rate of Ni-MOF-74 that can be synthesized by those methods is very low. Figure 4.1 shows the samples produced after the synthesis. Therefore, the synthesize method was being repeated for a few times in order to get enough amount of Ni-MOF-74 and Ni-MOF-74/GO @ Ni-MOF-74 to do characterization and experiment.

(a)

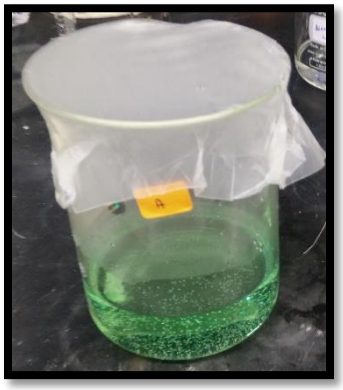

(b)

(c)

Figure 4.1 (a) Ni-MOF-74/GO @ Ni-MOF-74 before being dried in the vacuum oven. (b) Ni-MOF-74 after being dried in the vacuum oven. (c) Ni-MOF-74/GO @ Ni-MOF-74 after being dried in the vacuum oven.

The amount of Ni-MOF-74 synthesis and stored as follows:

Table 4.1 Amount of Ni-MOF-74 Synthesized

No.	***Batch***	***Amount of Ni-MOF-74 Synthesized (g)***
1	First	0.3204
2	Second	0.3682
3	Third	0.3814

During the synthesis process, the pores of the crystals are full of DMF (the solvent) molecules. When the crystals is being heated in the oven, the solvent molecules will be removed and leave the solid with accessible pore volume. The crystals are being centrifuge after heating in the oven in order the remove the unreacted particles.

4.2 CHARACTERIZATION OF Ni-MOF-74 AND Ni-MOF-74/GO

4.2.1 Thermogravimetric Analysis (TGA)

In Thermogravimetric Analysis (TGA) measurement, the exchange of materials between the samples the immediate surrounding has to be possible.

The TGA curve of synthesized Ni-MOF-74 at 60˚C is shown in Figure 4.2. The first weight loss produced around 122˚C. This can be due to the removal of solvent (DMF or water) from the cavities. The next major weight loss in the range of 400˚C to 650˚C corresponds to the organic ligand decomposition and therefore indicates the thermal stability of Ni-MOF-74 framework synthesized at 60˚C in air atmosphere (Botas et al., 2010)

(i) Sample of Ni-MOF-74 synthesized at 60°C

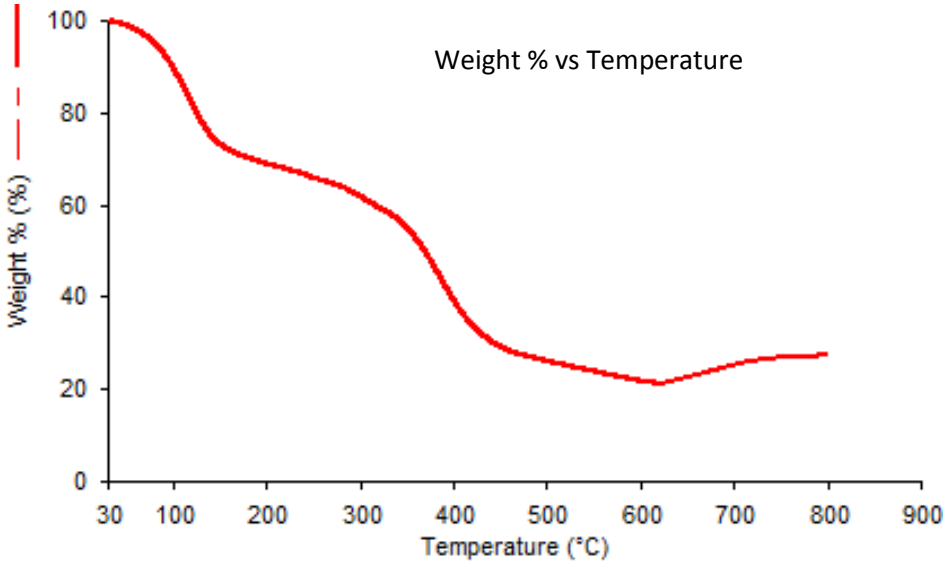

Figure 4.2 Weight % Temperature of Ni-MOF-74 sample synthesized at 60°C

(ii) Sample of Ni-MOF-74/GO (1st batch) synthesized

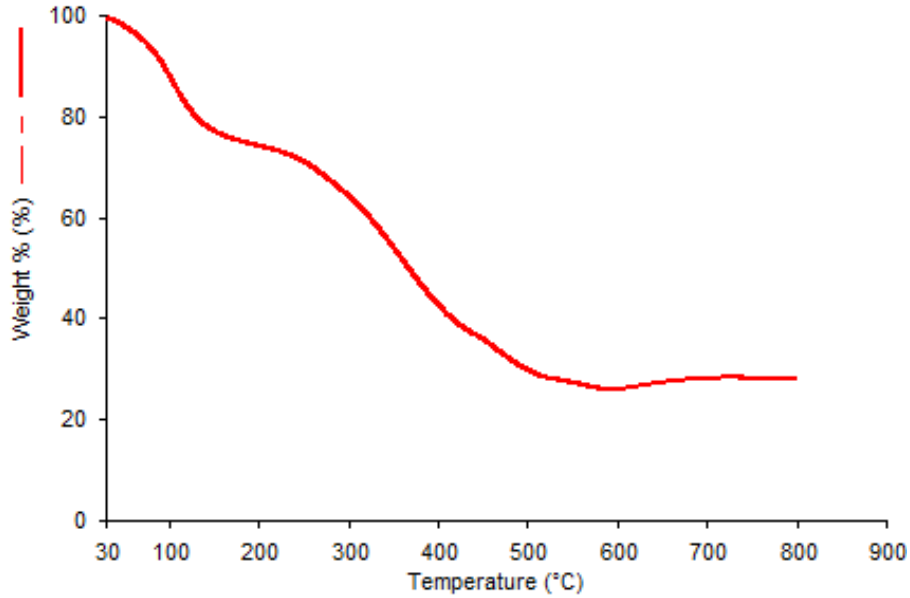

Figure 4.3 Weight % Temperature of Ni-MOF-74/GO for 1st batch sample

(iii) Sample of Ni-MOF-74/GO (2nd batch) synthesized

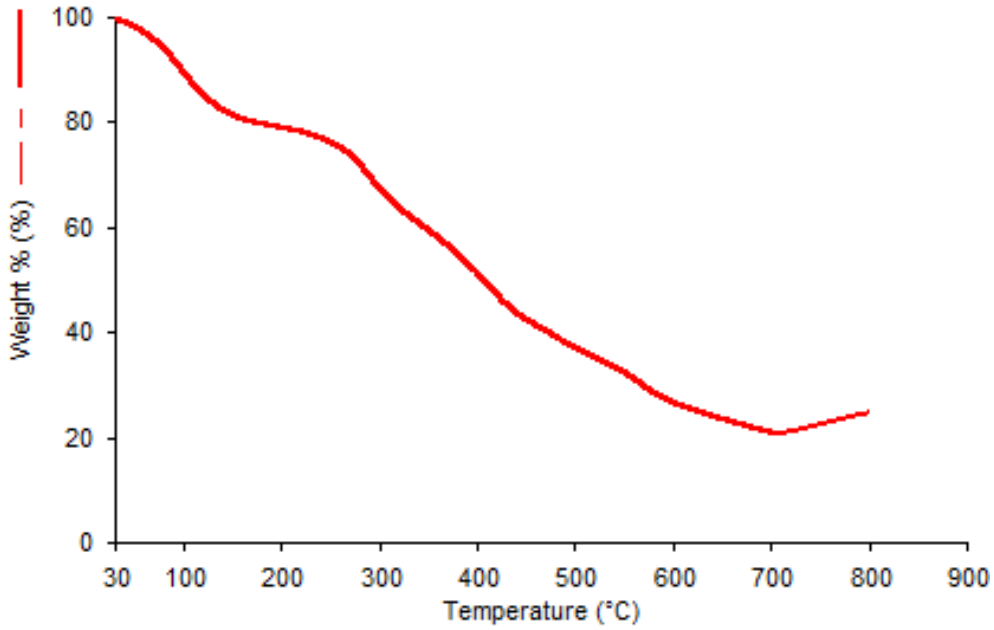

Figure 4.4 Weight % Temperature of Ni-MOF-74/GO for 2nd batch sample

The thermogravimetric curve in Figure 4.2 shows the thermal stability of Ni-MOF-74/GO powders precipitated in the autoclave bottom. There are two weight loss steps, i.e., the first weight loss, in line with 16% weight loss, occurs in the temperature range of 25– 230 °C corresponding to the loss of solvent molecules. The second weight loss, between 400 and 510 °C, can be ascribed to the decomposition of Ni-MOF-74/GO. The TG analysis shows that the structure of Ni-MOF-74/GO is stable up to 400 °C.

4.2.2 Scanning Electron Microscope (SEM)

Figure 4.5 displays the scanning electron microscopy (SEM) images of the Ni-MOF-74 sample prepared in this work.

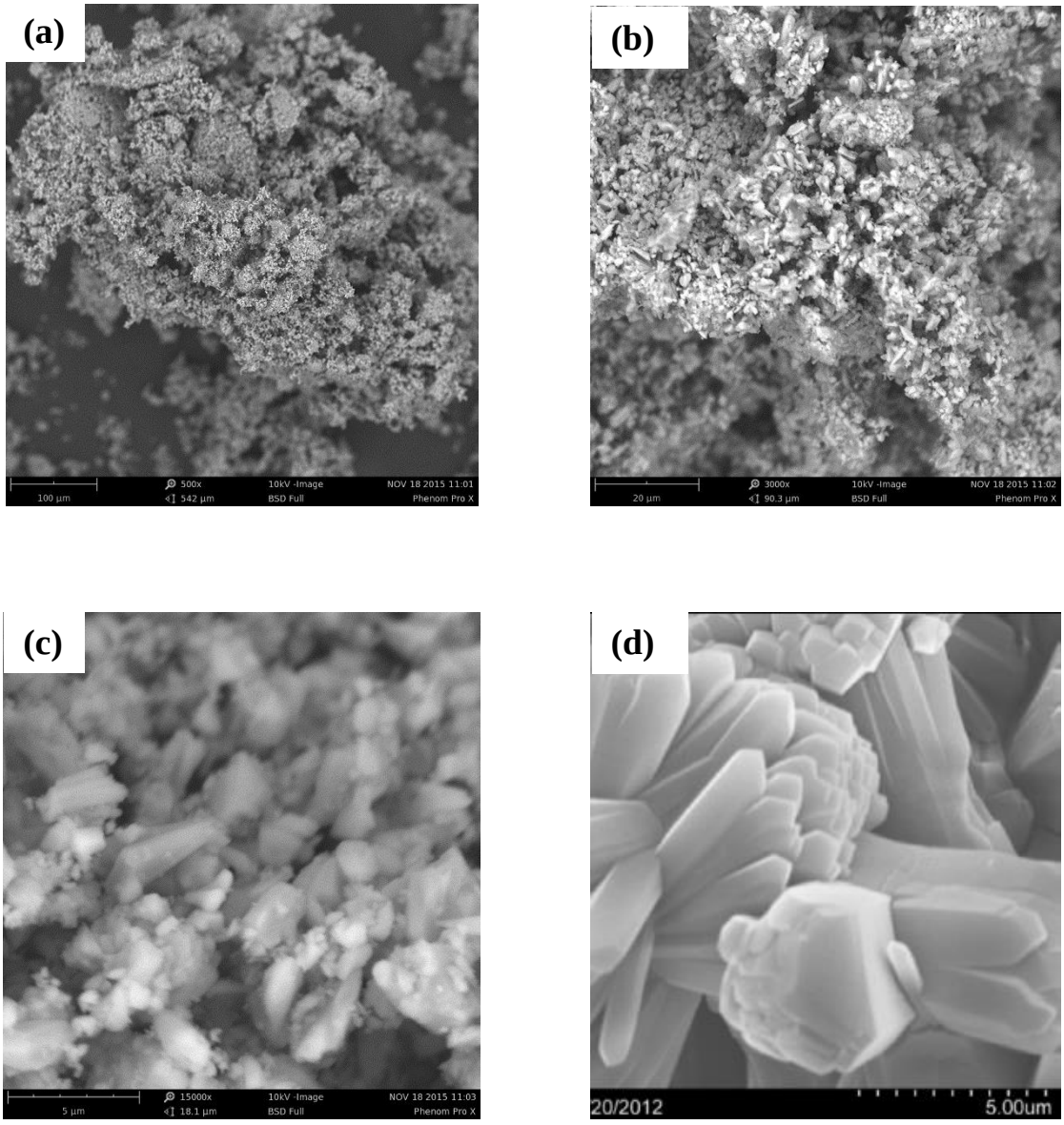

Figure 4.5 SEM of Ni-MOF-74 lab sample – Magnification of (a) 100µm (b) 20µm (c) 5µm (d) 5µm (X. Wu et al. , 201)

The crystals of Ni-MOF-74 (c) are quite similar in shape, small polyhedral aggregates with each other, just like flowers. The particle size of 1 is in the range of 1~3 μm; the particle size is more uniform, with an average size about 1 μm. The morphology for (d) is slightly similar, which is of column-like with length 3–5 μm.

The crystal size is determined by a combination effect of the nucleation rate and the crystal growth rate. i.e., small particles are obtained when the nucleation rate is higher than the crystal growth rate.

Figure 4.5 displays the scanning electron microscopy (SEM) images and particles size diameter of the Ni-MOF-74/GO samples prepared in this work.

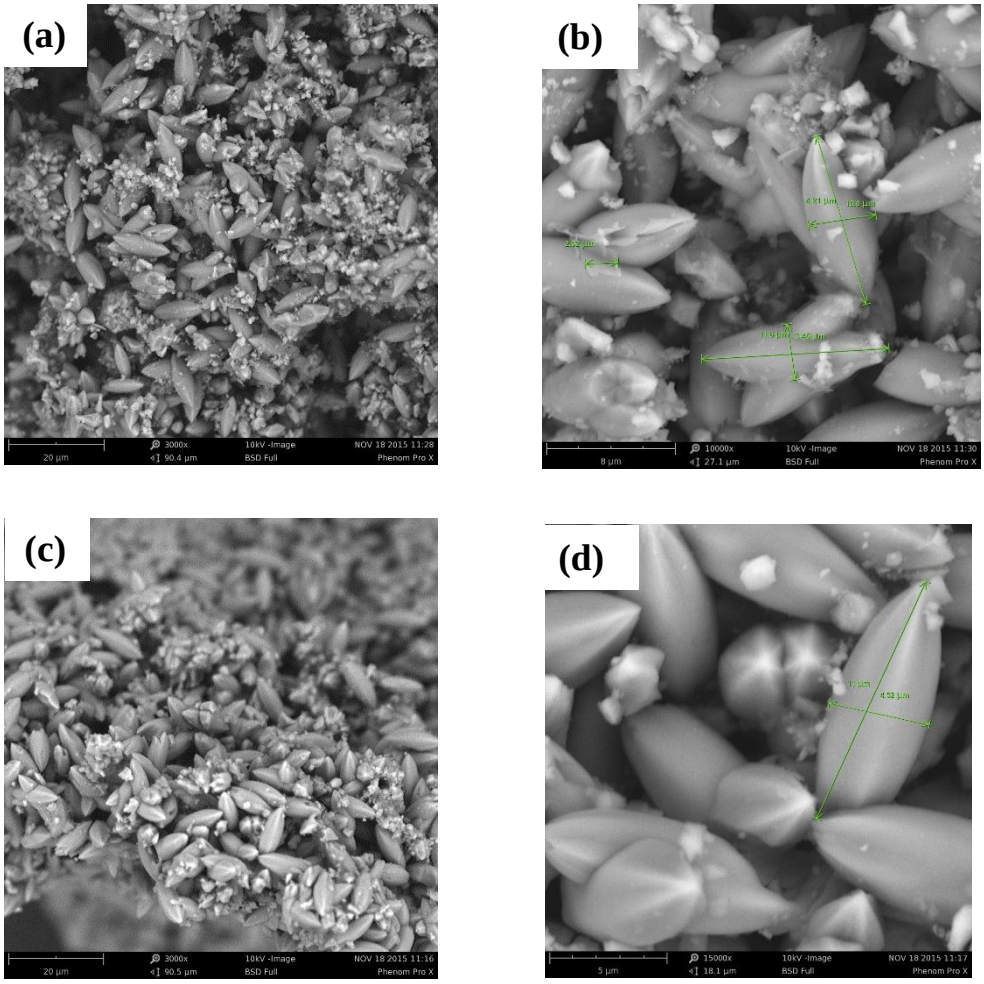

Figure 4.6 SEM of Ni-MOF-74/GO – Magnification of 1st batch (a) 20μm (b) 8μm; 2nd batch (c) 20μm (d) 5μm – Length of Particle (b) (d) 10μm-12μm

4.2.3 Energy Dispersive Spectroscopy (EDS)

EDS measurements were conducted for each sample, followed by SEM observations on the same Zeiss Ultra60 FE-SEM instrument at 10 kV with an Oxford EDS Super-X 50 mm2 detector, changing the aperture size from 30 to 120 µm and switching to high-current conditions. Three different point are selected to determine metal content homogeneity. Using mapping mode, the metals of interest were mapped to investigate metal distributions. Based on weight percentage shown that oxygen content is higher than Nickel (23.5%), Carbon (18.1%) and Nitrogen (11.3%).

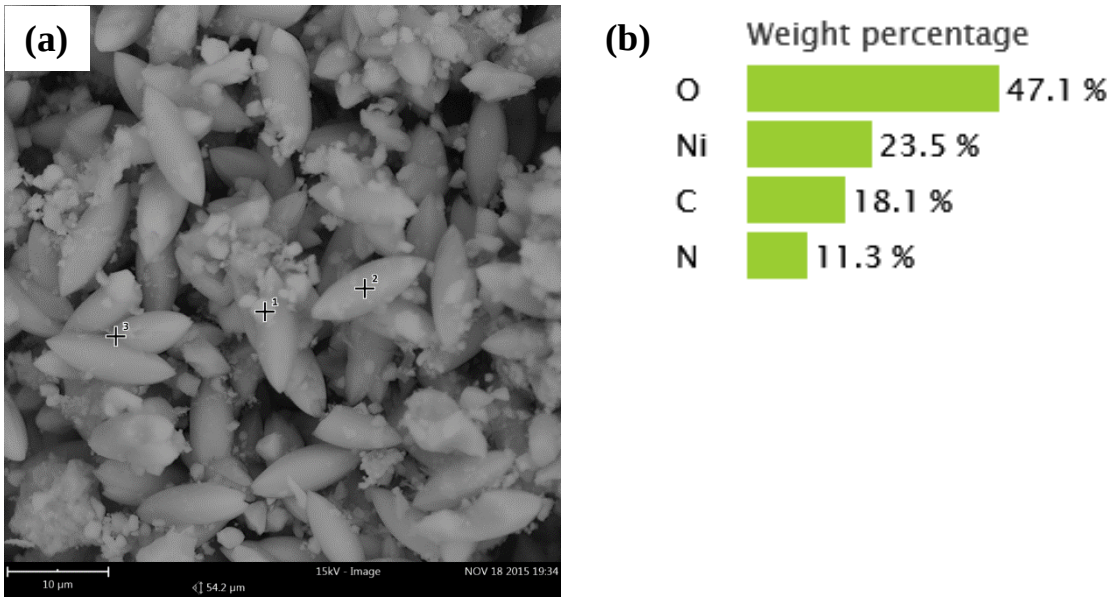

Figure 4.7 SEM images and EDS results of Ni-MOF-74/GO, (a) SEM image with specific EDS points, (b) EDS point mode percentage

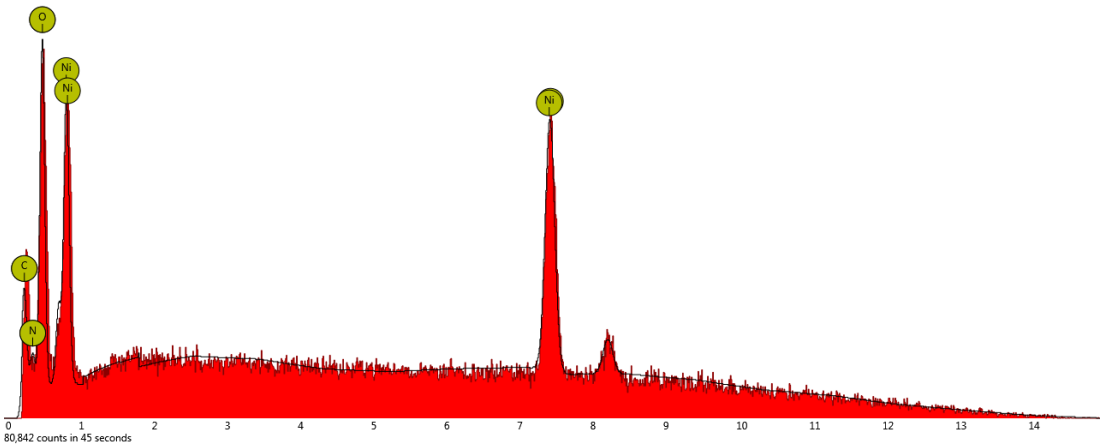

Figure 4.8 EDS spectrum of metal content in Ni-MOF-74/GO

EDS analyses were carried out using Ni-MOF-74/GO to investigate the distribution of metal ions in micrometer resolution. Based on Figure 4.8, the spectrum data shows that all metal are spread out within the area of the crystalline particles. This clearly demonstrates the presence of all 6 metals in the Ni-MOF-74/GO also show the presence of all expected metal ions, indicating that the samples are not a physical mixture of several different kinds of metal MOF-74 compounds.

4.2.4 Transmission Electron Microscope (TEM)

TEM images are obtained from Transmission Electron Microscope (TEM, Model: Zeiss Libra 200) with an accelerating voltage of 200kV.

A range from 59nm to 577.2nm of horizontal field width is used to observe the sample cell.

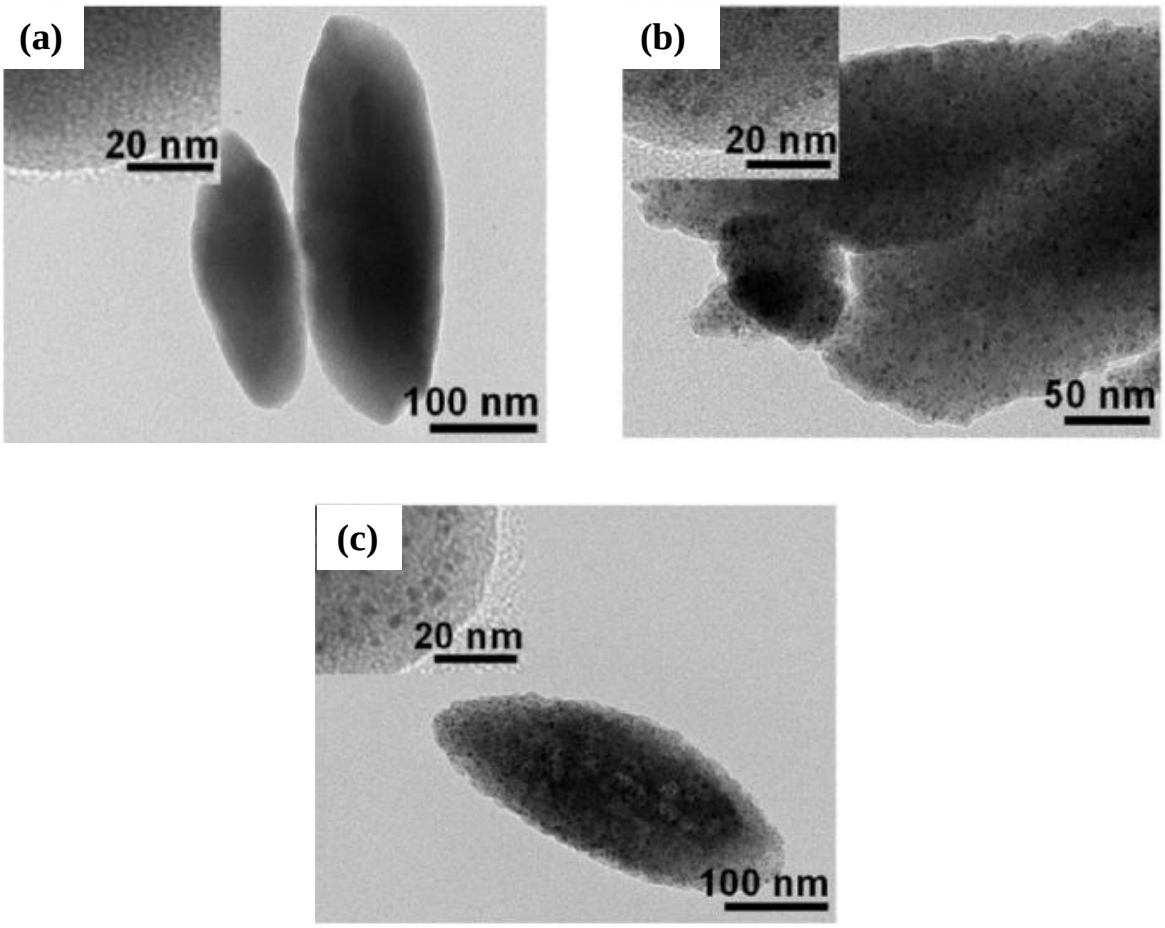

Figure 4.9 TEM of Ni-MOF-74 lab sample – Magnification of (a) 125k (b) 160k – Horizontal field width of (c) 577.2nm

The figures above are the representative TEM images observed for the Ni-MOF-74 samples. The images are taken at several magnifications such as 80000x, 125000x, and 160000x. TEM images provide information on the physical structure of the Ni-MOF-74 synthesized. The compound's morphology and porosity were observed at the nano-crystal level. It closely related to its adsorption characteristics.

Figure 4.9(a) and (c) are taken at different magnifications, at 125000x and 160000x respectively, showing structure of more like solid granular which agrees to the results showed in the paper of Megumi Mukoyoshi (2013). The particles in figure 4.7(b) display some porosity in their structure. Results of TEM in this study are similar as the results reported previously (Megumi Mukoyoshi, 2013).

4.2.5 Fourier Transform Infrared (FTIR) Spectroscopy

It is very important to identify and analyse the major characteristic of Ni-MOF-74 infrared spectrum. The spectra obtained from both the synthesized MOF-74 at 60˚C and 110˚C respectively were analyzed in this project according to absorption peaks. Refer Appendix for FTIR spectra results.

From the two graphs generated from FTIR analysis, both are showing the almost similar spectra. According to the table of Characteristic IR Absorptions, sharp peaks at 3400.28 cm-1 and 3411.97 cm-1 respectively indicate that both are having bond of O-H stretch or H-bonded. The functional groups are either alcohols or phenols. In addition, both compounds contain C-H stretch which represents functional group of alkanes (2926.37 cm-1 and 2927.57 cm-1 respectively).

In the frequency range from 2500 cm-1 to 2000 cm-1, several minor peaks can be observed from MOF-74 synthesized at 60˚C.

Figure 4.10 FTIR Spectra of Ni-MOF-74

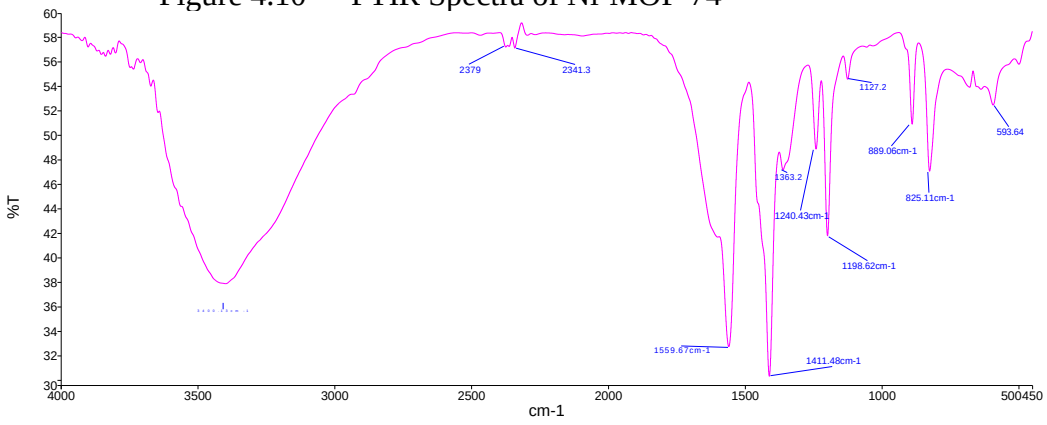

Figure 4.11 FTIR Spectra of Ni-MOF-74/GO

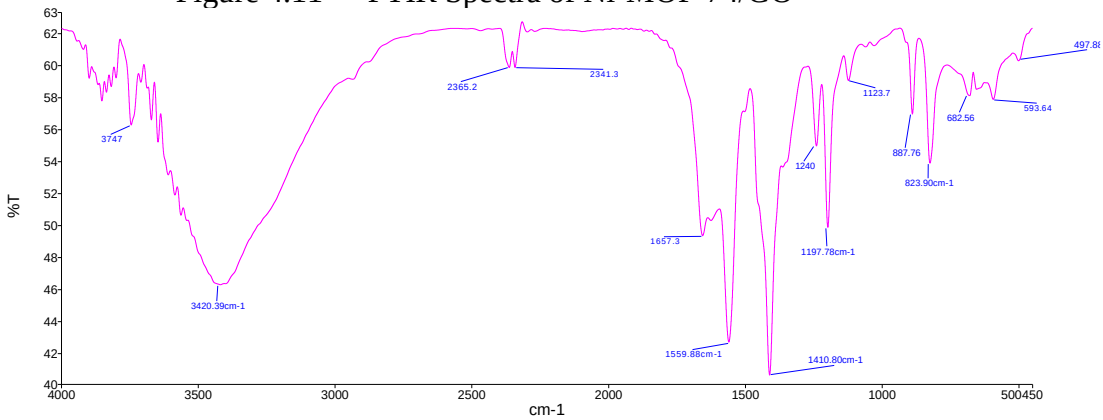

4.2.6 Carbon Dioxide Adsorption Capacity

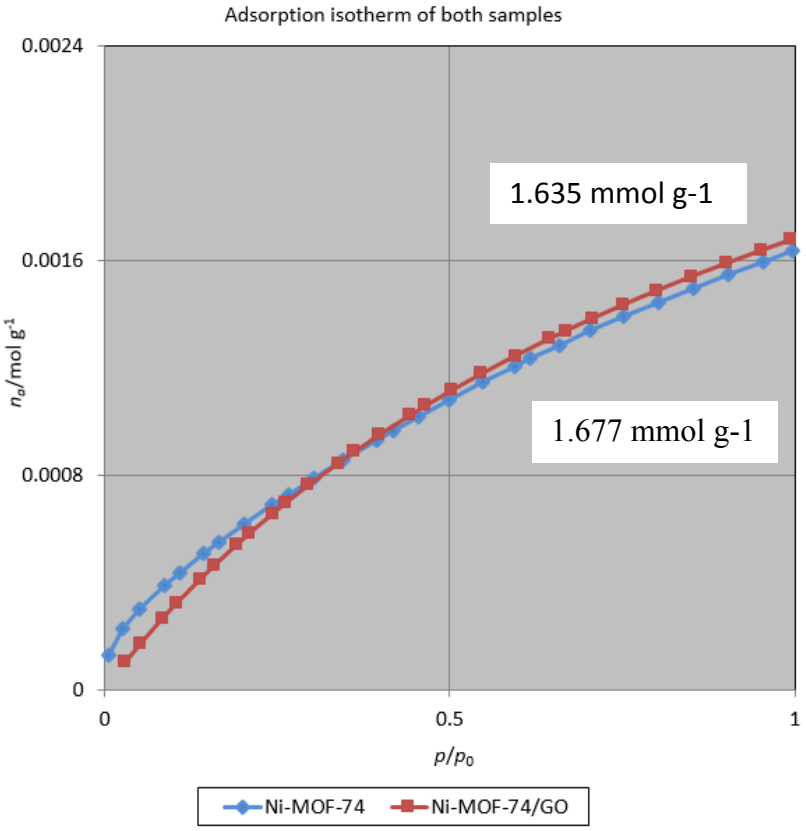

Figure 4.12 Ni-MOF-74 and Ni-MOF-74/GO Adsorption capacity

The CO_2 adsorption was conducted by using Belsorp Mini II. When comparing the graph the adsorption capacity of modified MOF-74 is slightly higher the MOF-74 adsorption capacity. We believe that the adsorption capacity will be higher when we increase the percentage of graphene modified MOF-274 beyond 10%.

The project is continued by increasing the percentage of MOF-74. The optimization of adsorption capacity will be achieved by increasing the percentage MOF-74 to 20%, 40% and 50%. This project still continues in order to investigate the capability of Modified MOF-74 towards CO_2 adsorption by increasing the percentage of MOF-74

CHAPTER 5
CONCLUSION AND RECOMMENDATION

As a conclusion, this project is important as it deals with overcoming the major weakness of metal organic frameworks, water stability and Ni-MOF-74 has a better adsorption among the MOFs. Project activities on synthesis of metal organic framework, Ni-MOF-74 as well as the characterization and modification were conducted to study on the characteristics and CO_2 adsorption on both samples in order to improve on CO_2 adsorption technology.

Ni-MOF-74 functionalized by Graphene Oxide (GO) is believed to be one of the effective ways to decrease the CO_2 concentration in the atmosphere due to its effective and better performance on CO_2 adsorption. Both samples are characterized by FTIR, TGA, FESEM, TEM and BET method.

As a recommendation, future work may be done to study on BET for N_2 adsorption isotherm analysis of Ni-MOF-74-GO and also study on manipulating the amount of GO grafted on Ni-MOF-74. Types of amine used in Ni-MOF-74 modification may be listed as one of the future works. The most important is the integration of MOF-74 applications in various industries.

REFERENCES

Botas, J.A., Calleja, G., Orcajo, M., Sánchez-Sánchez, M., Stolten, D. & Grube, T. (2010). Influence of Metal Doping of a MOF-74 Framework on Hydrogen Adsorption. *Report Nr.: Schriften des Forschungszentrums J\"ulich/Energy \& Environment*.

Britt, D., Furukawa, H., Wang, B., Glover, T. & Yaghi, O. (2009). Highly efficient separation of carbon dioxide by a metal-organic framework replete with open metal sites. *Proceedings of the National Academy of Sciences*, *106*(49), 20637-20640.

Chandan, Dey., Kundu, T., Bishnu P. Biswal, Mallicka, A. and Banerjeea, R. (2013). Crystalline metal-organic frameworks (MOFs): synthesis, structure and function. *Structural Science Crystal Engineering Materials*, *70*(1), 3-10.

Chen, B., Wang, X., Zhang, Q., Xi,X., Cai, J., Qi, H., Shi, S., Wang, J.,Yuan, Dan. & Fang, M. (2010). Synthesis and characterization of the interpenetrated MOF-5. *Journal of Materials Chemistry*, *20*(1).

Choi, S., Watanabe, T., Bae, T., Sholl, D. S. and Jones, C. W. (2012). Modification of the Ni/DOBDC MOF with amines to enhance CO2 adsorption from ultradilute gases. *The Journal of Physical Chemistry Letters*, *3*(9), 1136-1141.

Furukawa, H., Ko, N., Go, Y.B., Aratani, N., Choi, S.B., Choi, E., Yazaydin, A.O., Snurr, R.Q., Keeffe, M.O., Kim, J., Yaghi, O.M.: Ultra-high porosity in metal-organic frameworks. Science 329, 424–428 (2010)

I, Ahmed., NA, Khan., SH, Jhung. (2014). Graphite oxide/metal–organic framework (MIL-101): remarkable performance in the adsorptive denitrogenation of model fuels. *Inorganic chemistry*, *52*(24), 14155-14161

Gargiulo, N., Peluso, A., Aprea, P., Hua, Y., Filipovic, D., Caputo, D., and Eic, M.: A chromium-based metal organic framework as a potential high performance adsorbent for anaesthetic vapours. *RSC Adv*, *4*(2), 49478-49484 (2014)

Glover, T.G., Peterson, G.W., Schindler, B.J., Britt, D. & Yaghi, O. (2010). MOF-74 building unit has a direct impact on toxic gas adsorption. *Chemical Engineering Science*, *66*(2), 163-170.

Jeong, H. K., M. Gonzalez, M. C. McCarthy, and M. Shah. (2011). An Unconventional method for Metal-Organic Framework MOF Membranes with Enhanced Microstructure, Langmuir, 29(25), p7896-7902

Lee, J., Farha, O. K., Roberts, J., Scheidt, K. A., Nguyen, S. T., and Hupp, J. T. (2009). Metal-organic framework materials as catalysts. *Chem Soc Rev*, *38*(5), 1450-9

Liewellyn, P.L., Bourrelly, S., Serre, C., Vimont, A., Daturi, M., Iiamon, L.: High uptakes of CO2 and CH4 in mesoporous metalorfanic frameworks MIL-100 and MIL-101. Langmuir 24, 7245–7250 (2008)

Liu, Y.Y., Zeng, J.L., Zhang, J., Xu, F., Sun, L.X.: Improved hydrogen strorage in the modified metal-organic frameworks by hydrogen spillover effect. Int. J. Hydrogen Energy 32, 4005–4010 (2007)

Liu, J., Wang, Y., Benin, A.I., Jakubczak, P., Willis, R.R., Levan, M.D.: CO2/H2O adsorption equilibrium and rates on metalorganic frameworks: HKUST-1 and Ni/DOBDC. Langmuir 26, 14301–14307 (2010)

Liu, J., Thallapally, P.K., McGrail, B.P., Brown, D.R., Liu, J.: Process in adsorption-based CO2 capture by metal-organic frameworks. Chem. Soc. Rev. 41, 2308–2322 (2012)

Megumi, M., Hirokazu, K., Kusada, K., Mikihiro, H., Teppei, Y., Mitsuhiko, M., Jared, M., and Hiroshi, K.: Hybrid materials of Ni NP@MOF prepared by a simple synthetic method. *Chem. Commun.*, 2013, 51, 12463-12466

Millwar, A.R., Yaghi, O.M.: Metal-organic frameworks with exceptionally high capacity for storage of carbon dioxide at room temperature. J. Am. Chem. Soc. 127, 17998–17999 (2005)

Petit, C., Bandosz, T.J.: MOF-graphite oxide nanocomposites: surface characteriazation and ecaluation as adsorbents of ammonia. J. Mater. Chem. 19, 6521–6528 (2009a)

Petit, C., Bandosz, T.J.: MOF-graphite oxide composites: combing the uniqueness of grapheme layers and metal-organic frameworks. Adv. Mater. 21, 4753–4757 (2009b)

Petit, C., Bandosz, T.J.: Enhanced adsorption of ammonia on metalorganic framework/graphite oxide composites: analysis of surface interactions. Adv. Funct. Mater. 20, 111–118 (2010)

Petit, C., Mendoza, B., Bandoza, T.: Reactive adsorption of ammonia on Cu-based MOF/grapheme composites. Langmuir 26, 15302–15309 (2010)

Petit, C., Burress, J., Bandosz, T.J.: The synthesis and characterization of copper-based metal-organic framework/graphite oxide composites. Carbon 49, 563–572 (2011)

Rallapalli, P.B.S., Raj, M.C., Patil, D.V., Prasanth, P.K., Somani, R.S., Bajaj, H.C.: Activated carbon@MIL-101(Cr): a potential metal-organic framework composite material for hydrogen strorage. Int. J. Energy Res. 37, 746–753 (2013)

Rong, Li, J., Zhang, D., Chang, Z., Jiang Z., Zhang, H., Cheng, Q.: Fluorous Metal-Organic Frameworks with Enhanced Stability and High H_2/CO_2 Storage Capacities. 3312 (2013)

Sabouni, R., Kazemian, H., and Rohani, Sohrab.: Mathematical Modeling and Experimental Breakthrough Curves of Carbon Dioxide Adsorption on Metal Organic Framework CPM-5. *Environ. Sci. Technol.*, **2013**, *47* (16), pp 9372–9380

Schoenecker, P. (2012). High-throughput synthesis and application development of water-stable MOFs. Georgia Institute of Technology.

Suddik, A.C., Cote, A.P., Wong-Foy, A.G., O'Keeffe, M., Yaghi, O.M.: A metal-organic framework with a hierarchical system of pores and tetrahedral building blocks. Angew. Chem. Int. Ed. 45, 2528–2533 (2006)

Tranchemontagne, D.J., Hunt, J.R. & Yaghi, O.M. (2008). Room temperature synthesis of metal-organic frameworks: MOF-5, MOF-74, MOF-177, MOF-199, and IRMOF-0. *Tetrahedron, 64*(36), 8553-8557.

Uzun, A. & Keskin, S. (2014). Site characteristics in metal organic frameworks for gas adsorption. *Progress in Surface Science, 89*(1), 56-79.

Wang, X.*; Gao, W.-Y.; Luan, J.; Wojtas, L.; Ma, S. (2009). An Effective Strategy to Boost the Robustness of Metal-Organic Frameworks via Introducing Size-Matching Ligand Braces. *Chem. Commun*. 52, 1971-1974.

Wikipedia. (2014). Metal-organic framework. Retrieved February 18, 2014 from http://en.wikipedia.org/wiki/Metal-organic_framework

Wu, X., Bao, Z., Yuan, B., Wang, J., Sun, Y., Luo, H. & Deng, S. (2013). Microwave synthesis and characterization of MOF-74 (M = Ni, Mg) for gas 38 separation. *Microporous and Mesoporous Materials, 180,* 114-122.

APPENDICES

a) SEM image of spot 1 on Ni-MOF-74/GO

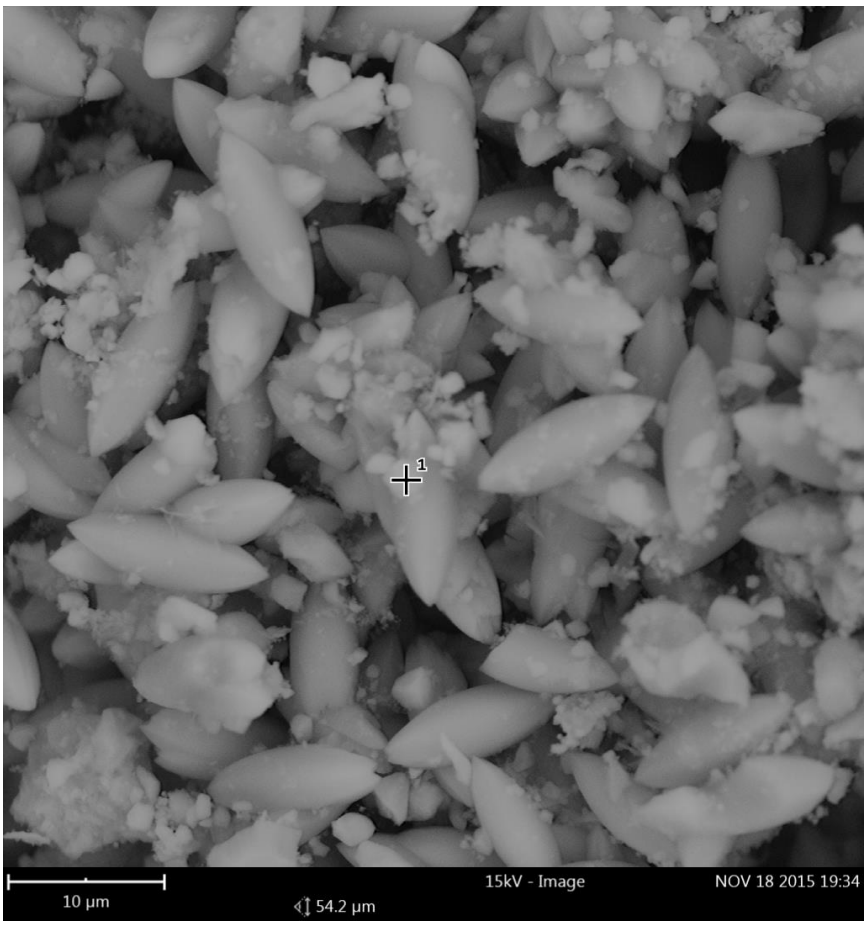

b) EDS spectrum of spot 1 on Ni-MOF-74/GO

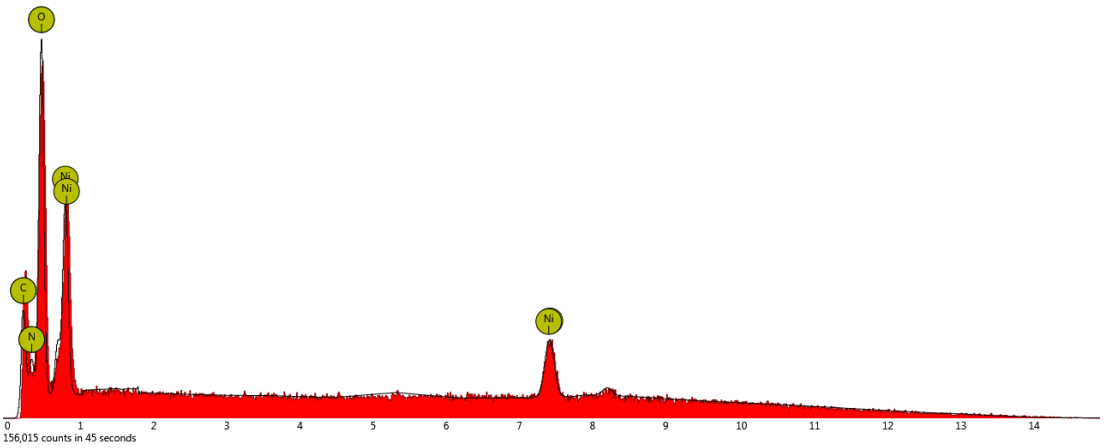

c) SEM image of spot 2 on Ni-MOF-74/GO

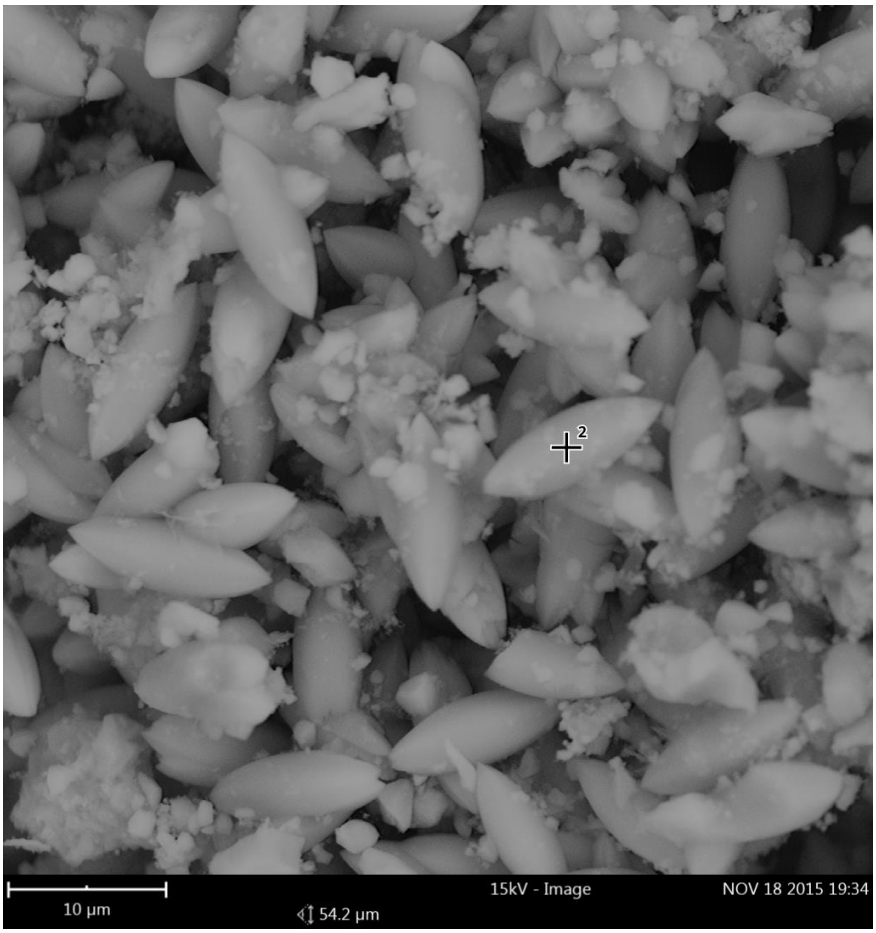

d) EDS spectrum of spot 2 on Ni-MOF-74/GO

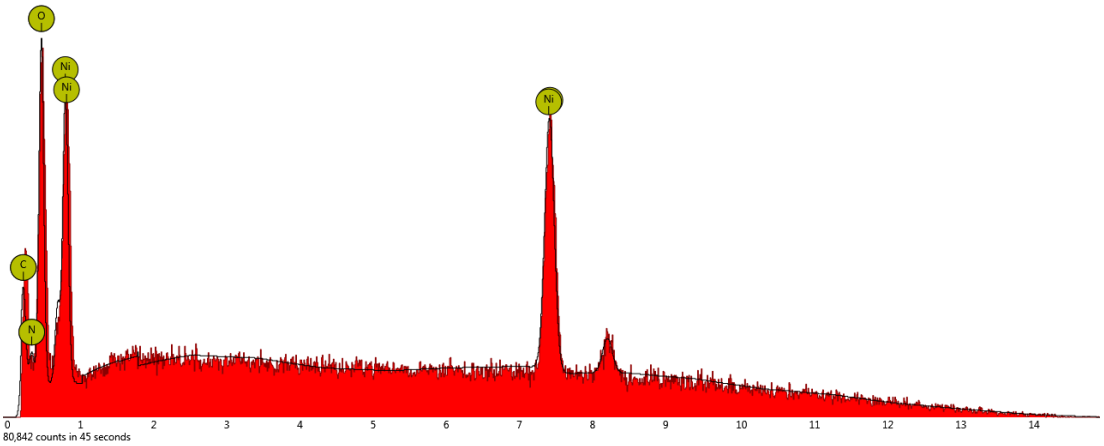

e) SEM image of spot 3 on Ni-MOF-74/GO

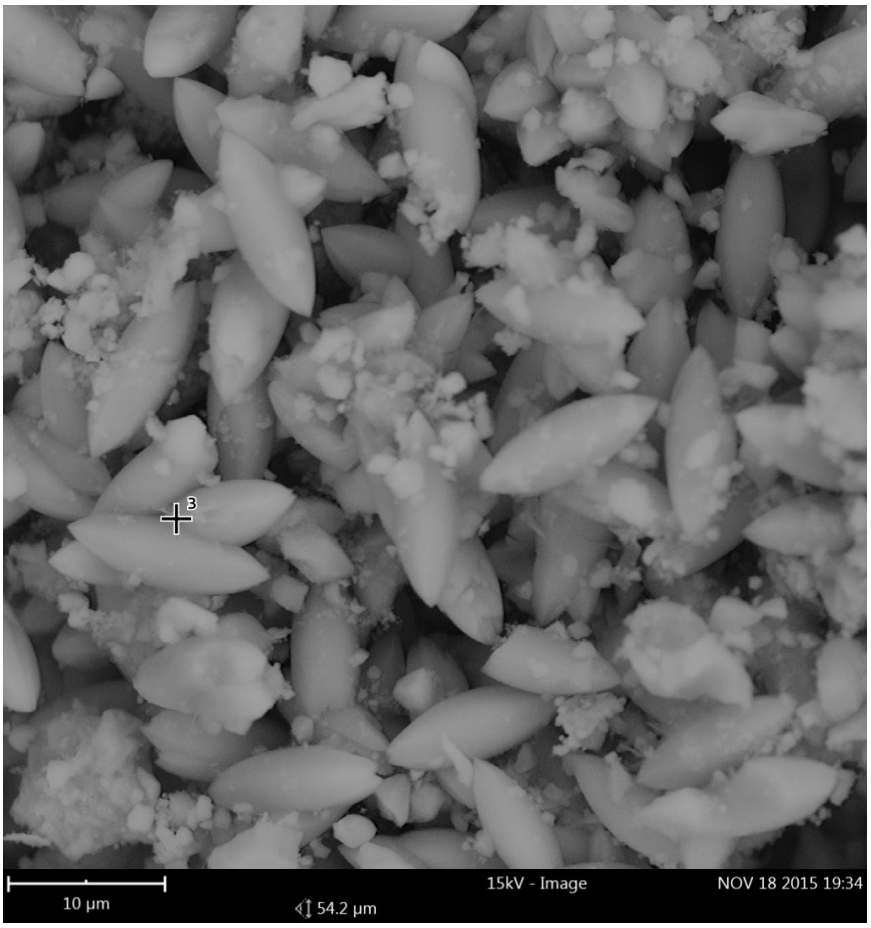

f) EDS image of spot 3 on Ni-MOF-74/GO

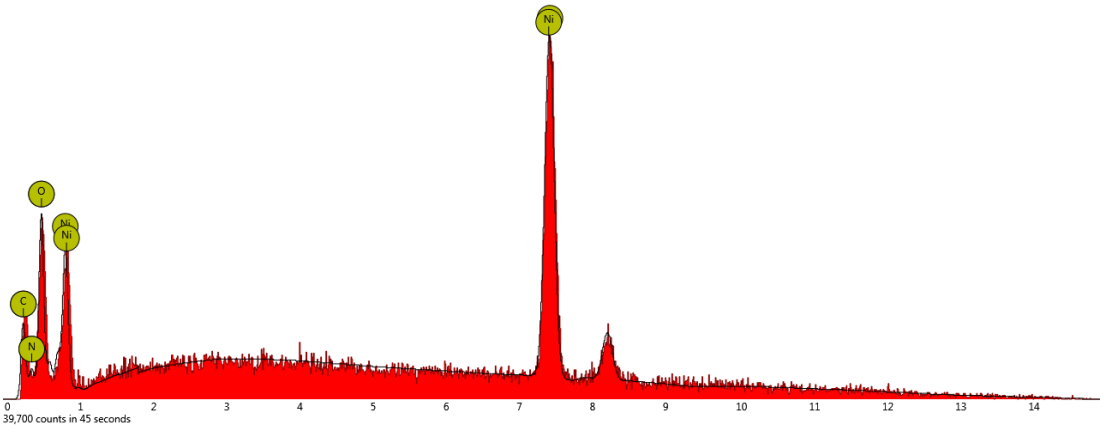

g) Fourier-transform infrared (FT-IR) spectra of Ni-MOF-74 and composites.

FTIR Spectra Table

Table of Characteristic IR Absorptions

frequency, cm^{-1}	*bond*	*functional group*
3640–3610 (s, sh)	O–H stretch, free hydroxyl	alcohols, phenols
3500–3200 (s,b)	O–H stretch, H–bonded	alcohols, phenols
3400–3250 (m)	N–H stretch	1°, 2° amines, amides
3300–2500 (m)	O–H stretch	carboxylic acids
3330–3270 (n, s)	–C≡C–H: C–H stretch	alkynes (terminal)
3100–3000 (s)	C–H stretch	aromatics
3100–3000 (m)	=C–H stretch	alkenes
3000–2850 (m)	C–H stretch	alkanes
2830–2695 (m)	H–C=O: C–H stretch	aldehydes
2260–2210 (v)	C≡N stretch	nitriles
2260–2100 (w)	–C≡C– stretch	alkynes
1760–1665 (s)	C=O stretch	carbonyls (general)
1760–1690 (s)	C=O stretch	carboxylic acids
1750–1735 (s)	C=O stretch	esters, saturated aliphatic
1740–1720 (s)	C=O stretch	aldehydes, saturated aliphatic
1730–1715 (s)	C=O stretch	α, β–unsaturated esters
1715 (s)	C=O stretch	ketones, saturated aliphatic
1710–1665 (s)	C=O stretch	α, β–unsaturated aldehydes, ketones
1680–1640 (m)	–C=C– stretch	alkenes
1650–1580 (m)	N–H bend	1° amines
1600–1585 (m)	C–C stretch (in–ring)	aromatics
1550–1475 (s)	N–O asymmetric stretch	nitro compounds
1500–1400 (m)	C–C stretch (in–ring)	aromatics
1470–1450 (m)	C–H bend	alkanes
1370–1350 (m)	C–H rock	alkanes
1360–1290 (m)	N–O symmetric stretch	nitro compounds
1335–1250 (s)	C–N stretch	aromatic amines
1320–1000 (s)	C–O stretch	alcohols, carboxylic acids, esters, ethers
1300–1150 (m)	C–H wag ($–CH_2X$)	alkyl halides
1250–1020 (m)	C–N stretch	aliphatic amines
1000–650 (s)	=C–H bend	alkenes
950–910 (m)	O–H bend	carboxylic acids
910–665 (s, b)	N–H wag	1°, 2° amines
900–675 (s)	C–H "oop"	aromatics
850–550 (m)	C–Cl stretch	alkyl halides
725–720 (m)	C–H rock	alkanes
700–610 (b, s)	–C≡C–H: C–H bend	alkynes
690–515 (m)	C–Br stretch	alkyl halides

m=medium, w=weak, s=strong, n=narrow, b=broad, sh=sharp